Acta Crystallographica Section D
Biological Crystallography
ISSN 0907-4449

The first crystal structure of a gramicidin complex with sodium: high-resolution study of a nonstoichiometric gramicidin D–NaI complex

A. Olczak,[a]* M. L. Główka,[a] M. Szczesio,[a] J. Bojarska,[a] Z. Wawrzak[b] and W. L. Duax[c,d]

[a]Institute of General and Ecological Chemistry, Technical University of Łódź, Żeromskiego 116, 90-924 Łódź, Poland, [b]Northwestern University Center for Synchrotron Research, Life Sciences Collaborative Access Team, Department of Biochemistry, Molecular Biology and Cell Biology, Northwestern University, Argonne, Illinois 60439, USA, [c]Hauptman–Woodward Medical Research Institute, Buffalo, NY, USA, and [d]State University of New York at Buffalo, Buffalo, NY, USA

Correspondence e-mail: olczakan@p.lodz.pl

Received 11 February 2010
Accepted 26 May 2010

PDB Reference: gramicidin D–NaI complex, 3l8l.

The crystal structure of the nonstoichiometric complex of gramicidin D with NaI has been studied using synchrotron radiation at 100 K. The limiting resolution was 1.25 Å and the *R* factor was 16% for 19 883 observed reflections. The general architecture of the antiparallel two-stranded gramicidin dimers in the studied crystal was a right-handed antiparallel double-stranded form that closely resembles the structures of other right-handed species published to date. However, there were several surprising observations. In addition to the significantly different composition of linear gramicidins identified in the crystal structure, including the absence of the gramicidin C form, only two cationic sites were found in each of the two independent dimers (channels), which were partially occupied by sodium, compared with the seven sites found in the RbCl complex of gramicidin. The sum of the partial occupancies of Na^+ was only 1.26 per two dimers and was confirmed by the similar content of iodine ions (1.21 ions distributed over seven sites), which was easily visible from their anomalous signal. Another surprising observation was the significant asymmetry of the distributions and occupancies of cations in the gramicidin dimers, which was in contrast to those observed in the high-resolution structures of the complexes of heavier alkali metals with gramicidin D, especially that of rubidium.

1. Introduction

Gramicidin was isolated by Hotchkiss & Dubos (1941) from tyrothricin, a toxic substance produced by the soil bacterium *Bacillus brevis* (Dubos, 1939; Hotchkiss & Dubos, 1940). Gramicidin appears to be a mixture of six linear pentadecapeptides modified at both ends (gramicidin D) and one cyclic decapeptide called gramicidin S. The six linear gramicidins differ at two positions, which may be occupied by either valine (Vg) or isoleucine (Ig) at position 1 (Ishii & Witkop, 1963; Ramachandran, 1963) and by either tryptophan (gA), phenylalanine (gB) or tyrosine (gC) at position 11 (Fig. 1). Common gramicidin D contains about 80% gramicidin A, 5% gramicidin B and 15% gramicidin C (Sarges & Witkop, 1965). However, the content of Val at position 1 may vary from 80% to 95% (Sarges & Witkop, 1964; Gross & Witkop, 1965).

***N*-formyl–*X*1–Gly2–Ala3–D-Leu4–Ala5–D-Val6–Val7–D-Val8–Trp9–D-Leu$_{10}$–*Y*11–D-Leu12–Trp13–D-Leu14–Trp15–ethanolamine**

*X*1 is Val in Vg and Ile in Ig

*Y*11 is Trp in gA, Phe in gB and Tyr in gC

Figure 1
Gramicidin.

© 2010 International Union of Crystallography
Printed in Singapore – all rights reserved

Table 1
Crystal data, solution and refinement statistics (PDB code 3l8l).

Crystal data for gD–NaI complex	
Formula of main component (gA)	$C_{99}N_{20}O_{17}H_{140}$
Molecular weight (gA) (Da)	1882.3
Formula of asymmetric unit	$C_{394.5}N_{79}O_{68}H_{556}$, $Na_{1.26}$, $I_{1.21}$, (18.5 H_2O), (2 MeOH)
Crystal system	Orthorhombic
Formula units Z (Z')	16 (4)
Crystal dimensions (mm)	0.33 × 0.31 × 0.15
Linear absorption coefficient (mm^{-1})	0.21
Radiation source and wavelength (Å)	Synchrotron; 0.918
Crystallographic data-collection details	
Space group	$P2_12_12_1$
Unit-cell parameters (Å)	a = 29.82, b = 31.23, c = 51.67
Unit-cell volume ($Å^3$)	48148
No. of measured reflections	671011
No. of unique reflections	24628
No. of observed reflections (>4σ)	19883
Resolution range (Å)	1.25–26.74
Overall completeness (%)	96.00
Refinement statistics and other details	
Restraints	6735
Resolution range (Å)	26.74–1.25
Final R_{free} (%)	16.21
Final R_1 (%)	15.28
Final R_1, all data (%)	16.36
wR^2	0.4065
Goodness of fit (GooF)	1.017
Flack parameter	0.06 (0.03)
$\Delta\rho$ (max, min) (e $Å^{-3}$)	0.78, −0.37

An important factor influencing the antibacterial function of linear gramicidin is the alternate order of D- and L-amino acids (Fig. 1).

Linear gramicidin is a natural antibiotic against Gram-positive species. The molecule functions by creating a pore in the outer membrane (Hotchkiss, 1944) that is capable of transporting monovalent cations (for example, ions of the first-group metals, Tl^+, NH_4^+ and H_3O^+; Pressman, 1965). Gramicidin adopts different dimer conformations depending on its environment (Chen *et al.*, 1996). The two basic types are a single-stranded head-to-head single helix (HHSH) and a double-stranded double helix (DSDH), with the latter being observed preferentially in isotropic environments (Urry, 1971; Urry *et al.*, 1971; Veatch *et al.*, 1974; Veatch & Blout, 1974).

In the solid state two distinct conformational states have been reported: a cation-free left-handed antiparallel double-stranded dimer (Langs, 1988; Langs *et al.*, 1991) and an ion-complexed right-handed antiparallel double-stranded dimer (Burkhart, Li *et al.*, 1998; Główka *et al.*, 2005; Duax *et al.*, 2003). NMR data have been reported that confirm the existence of these forms in solution. Although a left-handed antiparallel structural model has been reported for the Cs^+- and K^+-complex forms (Wallace & Ravikumar, 1988; Wallace *et al.*, 1990; Doyle & Wallace, 1997), the diffraction intensity data supporting the model have not been deposited and no evidence of a Cs^+ or K^+ complex in solution has been reported.

The importance of sodium ions in cell function prompted us to study the high-resolution molecular structure of gramicidin in complex with sodium. The presence of iodine in the crystal allowed us to use anomalous scattering to reliably locate the iodine ions, which in turn allowed a more accurate determination of the sodium-ion content. As in our previous studies (Główka *et al.*, 2005; Olczak *et al.*, 2007), we used wild-type gramicidin D for crystallization in order to acquire additional data on the possible role of heterodimers in the nucleation of gramicidin crystals and the solvent effect on crystal composition (Burkhart, Gassmann *et al.*, 1998).

Table 2
Heterogeneity of gramicidin D complexes (%).

The composition of the gD used in the crystallization was ∼80% gA, ∼5% gB and ∼15% gC (Sarges & Witkop, 1965). Dimer I consists of strands 100 and 200, while dimer II consists of strands 300 and 400. The order of the strands has been changed to highlight the similarities and differences between them.

	gD–NaI			gD–RbCl†			gD–KI‡		
Strand	gA	gB	gC	gA	gB	gC	gA	gB	gC
100	100	—	—	100	—	—	75	—	25
300	100	—	—	100	—	—	74	—	26
200	61	39	—	77	—	23	50	15	35
400	62	38	—	81	—	19	70	12	18

† As determined from the X-ray structure at 1.14 Å resolution (Główka *et al.*, 2005), in which no gB or Ig was detected. ‡ As determined from the X-ray structure at 0.80 Å resolution (Olczak *et al.*, 2007).

2. Materials and methods

2.1. Crystallization and data collection

Commercially available gramicidin D (Sigma) was batch-crystallized using a mixture of NaI and methanol. Crystals were cryocooled by immersion in liquid nitrogen after soaking them for a few seconds in glycerol cryoprotectant. Diffraction data were collected on the 5-ID beamline of DND-CAT at the Advanced Photon Source, Argonne, Illinois, USA using a 165 mm MAR CCD detector and were processed with the *HKL* software package (Otwinowski & Minor, 1997). Table 1 shows a summary of data collection.

2.2. Structure solution and refinement

The previously published KI complex (Olczak *et al.*, 2007) was used as a starting model for refinement *via* conjugate-gradient least-squares (CGLS) fitting with the *SHELX*97 package (Sheldrick, 2008; Table 1). Solvent positions, ion positions and peptide were determined using anisotropic least-squares refinement, except for side-chain disorder which was refined isotropically with manual adjustment. The occupancy factors of Na^+ cations, I^- anions and water molecules were unrestricted during refinement, while the occupancy sums of multiple side-chain conformations were constrained to unity. Engh & Huber (1991) restraints on bond distances and angles were used in refinement.

3. Results and discussion

3.1. Heterogeneity of the gramicidin

The crystal form utilized in this study contained four independent gramicidin molecules in the asymmetric unit. The four monomers form two pairs of right-handed helical strands

Table 3
Gramicidin channel content in gD–NaI complex.

	H_2O		Na^+		I^-	
	Content	Sites	Content	Sites	Content	Sites
Channel I	5.02	11	0.65	2		
Channel II	5.59	17	0.61	2		
Outside the channels	7.88	14			1.21	7
Total	18.49 (0.35)	42	1.26 (0.13)	4	1.21 (0.04)	7

	H_2O/Na	Na/I
Channel I	7.66	
Channel II	9.24	
Overall		1.04

intertwined in an antiparallel fashion. Although the gramicidin D used for crystallization was reported to be a mixture of 80–85% gA, 4–6% gB and 10–16% gC (Sigma–Aldrich), the relative proportions of the three forms in the crystal were quite different (Table 2). This ratio also differed from that found in our previous high-resolution studies on gramicidin D complexed with alkali halides (Główka *et al.*, 2005; Olczak *et al.*, 2007).

The three published gramicidin D complexes follow a pattern in their relative proportion of gramicidin forms and dimers (Table 2). Although both dimers and their equivalent strands (100 and 300, 200 and 400) have very similar compositions, the two strands forming each dimer (100 with 200 and 300 with 400) differ significantly. The only exception is the content of gA and gC in strands 200 and 400 in the potassium iodide complex (Olczak *et al.*, 2007). The most striking difference in composition between the three known gramicidin complexes is the reduced heterogeneity of strands 100 and 300, which consist of either pure form A (in the NaI and RbCl complexes) or at least a higher content of gA in strand 400 in the KI complex compared with strand 200 (Table 2). Some of the components found in the crystal vary dramatically from the starting gD composition. For example, there is no trace of gC in the NaI-complex crystal (gD usually consists of about 15% gC), while the contents of gB in strands 200 and 400 are almost 40% (Table 2) compared with 5% in the starting material (gD).

It is not easy to point out the reasons for the varied composition in these three crystal complexes containing different ions and crystallized from different solvents. The varied solvent content is thought to possibly be an important factor (Burkhart, Gassmann *et al.*, 1998).

3.2. Gramicidin dimer contents: sodium/water discrimination

The final refined model of the structure consists of 42 water sites, four Na^+-ion sites, seven I^--ion sites (Table 3) and three methanol sites. The overall contents of ions was 1.26 for Na^+ and 1.21 for I^-, *i.e.* significantly less than in the rubidium complex structure (Główka *et al.*, 2005) and slightly more than in the potassium complex structure (Olczak *et al.*, 2007).

Partial occupancy made it very difficult to distinguish waters from sodium ions during refinement. To solve the problem, we performed a careful analysis of electron density in the channel in conjunction with analysis of temperature and the occupancy factors of the ions and water molecules. We were able to

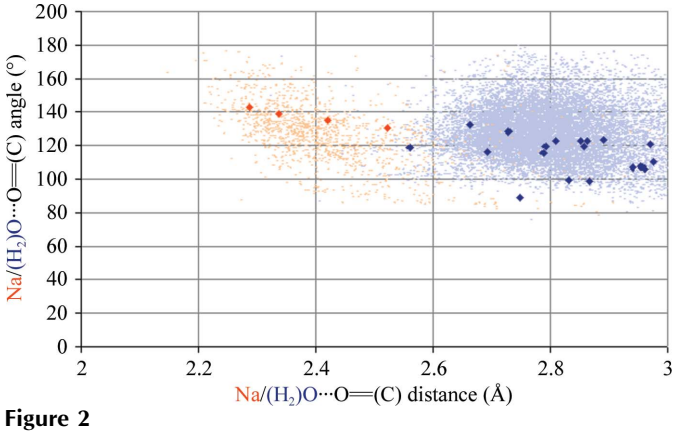

Figure 2
Scattergram of distances between water molecules or sodium ions and carbonyl O atoms *versus* C=O···*X*(O or Na) angles as found in the CSD (Allen, 2002). The large diamonds mark contacts found in the studied gramicidin structure (red, sodium ions; blue, water molecules).

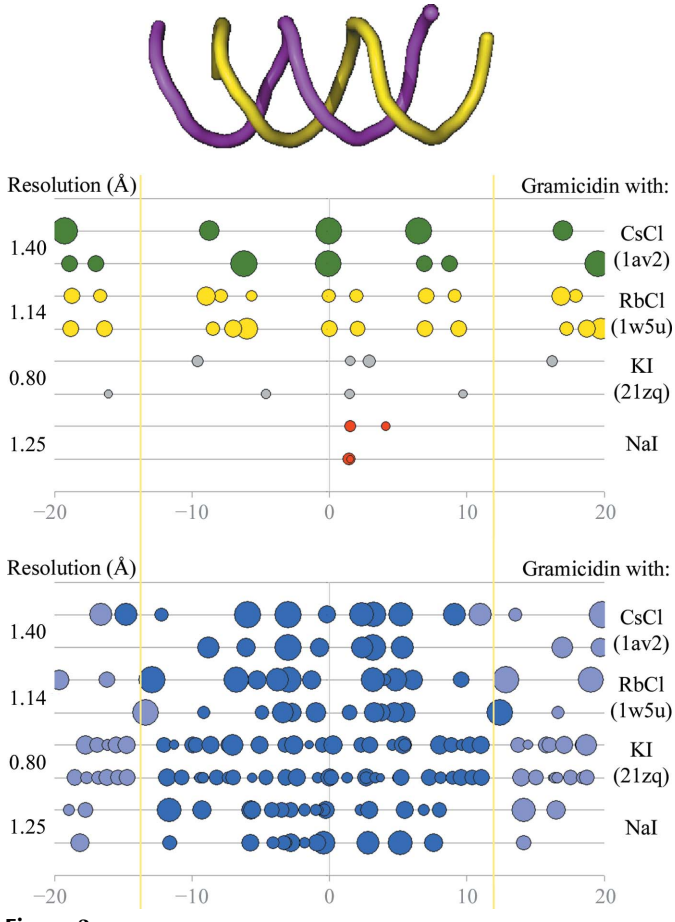

Figure 3
Distributions of cations and waters in the gramicidin dimers (channels), shown along the channel axis, for our gramicidin structure and PDB entries 1w5u (Główka *et al.*, 2005), 2izq (Olczak *et al.*, 2007) and 1av2 (Burkhart, Gassmann *et al.*, 1998). The areas of the circles are proportional to the occupancy factors.

Table 4
Geometry of Na···carbonyl contacts for Na···O distances less than 3.7 Å.

Contacts with Na—O—C angles less than 110° (which refer to cases in which a cation interacts with the π electrons of a carbonyl bond rather than with a lone pair of the O atom) are italicized and respective values in relation to the center of the carbonyl bond (indicated by *X*) are given.

Na^+ No.	Occupancy	B_{eq} (Å^2)	Residue	Na···O (Å)	Na···O=C (°)	Na···*X* (Å)	Na···*X*···O (°)
1	0.160	17.46	108	2.34	139.3	2.85	32.4
			206	2.70	117.2	3.03	52.4
			208	*3.23*	*87.4*	*3.26*	*81.8*
2	0.495	17.00	206	2.52	129.9	2.95	40.9
			108	2.58	125.8	3.00	44.3
			110	*3.17*	*88.8*	*3.21*	*80.3*
11	0.218	18.14	310	2.29	142.7	2.79	29.8
			404	2.70	142.6	3.21	30.7
			406	*3.26*	*90.3*	*3.32*	*79.3*
12	0.387	13.69	406	2.42	135.1	2.89	36.2
			308	2.66	130.7	3.10	40.5
			310	*3.00*	*94.4*	*3.11*	*74.4*

Table 5
Occupancies (and their sums) and atomic displacement parameters of ions, water and methanol as found in this study.

I	Occupancy	B_{eq} (Å^2)	HOH	Occupancy	B_{eq} (Å^2)	MeOH	Occupancy
21	0.27	21.44	81	0.73	30.36	501	1.00
22	0.42	13.62	82	0.58	12.74	502	0.46
23	0.08	12.59	83	0.40	11.63	503	0.50
24	0.10	15.12	84	0.40	14.88		
25	0.12	23.66	85	0.90	28.62		
26	0.09	23.91	86	0.36	24.45		
27	0.13	26.55	87	0.50	21.67		
			88	0.98	22.52		
			89	0.40	22.98		
			90	0.40	31.20		
			91	0.60	38.11		
			92	0.40	41.15		
			93	0.75	44.03		
			94	0.48	25.71		
Sum	1.21			7.88			1.96
B_{av} (Å^2)		19.56			26.43		

largely differentiate the binding sites by examining distances to adjacent carbonyl O atoms and comparing these with known (C=)O···Na^+ and (C=)O···O(water) contacts in the Cambridge Structural Database (CSD; Fig. 2). Also, the uniformity of Na^+···carbonyl contact geometry, of which two contacts are always Na^+···O and one is Na^+···π type (Table 4), confirms our identification, as well as the small final difference of only 4% between the total content of sodium ions and their I^- counterions, the occupancies of which were refined freely.

3.3. Distribution of cations and waters in the double-stranded gramicidin channel

Fig. 3 shows large differences in the distributions of cations and waters in the gramicidin antiparallel double-stranded dimers, as found in the crystal structures of right-handed gramicidin complexes, especially those resolved at high resolution (Główka *et al.*, 2005; Olczak *et al.*, 2007; Burkhart, Gassmann *et al.*, 1998). There is a distinct difference between the distributions of light (K^+ and Na^+) and heavy (Cs^+ and Rb^+) alkali metals. The most symmetrical distribution of cations in the gramicidin channel was observed in the gD–RbCl structure, while light-alkali cations show significant asymmetry in this respect (Fig. 3).

We believe that the explanation lies in the mechanism of M^+–gramicidin complex and dimer formation in solution, which is an equilibrium with other forms observed using NMR (Chen *et al.*, 1996). When the dimer begins to close up, a monovalent cation may be trapped inside. In the case of large cations such as Cs^+ or Rb^+, which are hydrated less strongly than Na^+ and K^+, the process takes place at an earlier stage during closure, when there is also a higher probability of the second ion being trapped at the other end, enabling a symmetric distributions of ions. On the other hand, usually only one end of the dimer is accessible to Na^+ or K^+, leading to the observed asymmetry in the crystal structures of gramicidin complexes with these cations (Fig. 3).

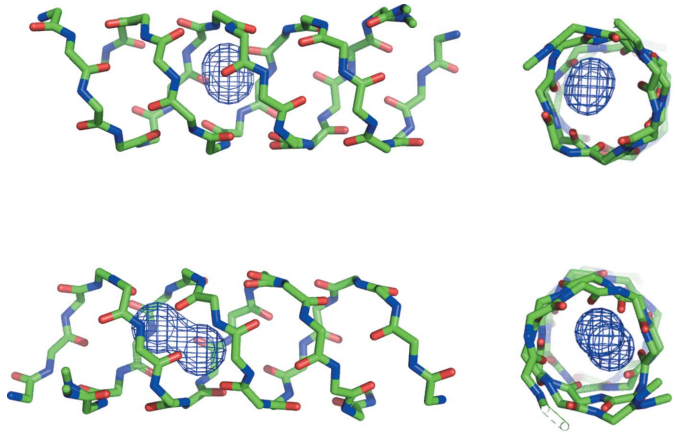

Figure 4
Na^+-ion positions (van der Waals surfaces) of the gD–NaI complex.

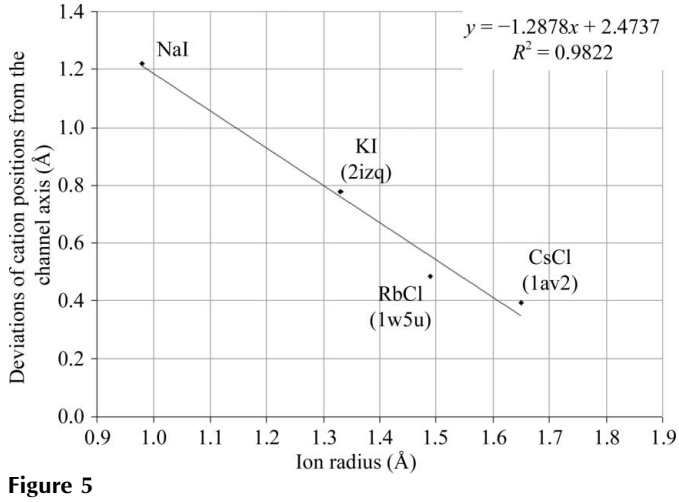

Figure 5
Deviations of cation positions as found in the gramicidin dimers in the crystal structures of complexed gramicidin from the channel axis in relation to ion size. [PDB entry 1w5u, Główka *et al.* (2005); PDB entry 2izq, Olczak *et al.* (2007); PDB entry 1av2, Burkhart, Gassmann *et al.* (1998).]

Table 6
Geometry of iodide contacts.

Owing to the partial occupancies of waters and iodides, only contacts with Trp residues need to meet common geometrical requirements. (I···N distances of less than 4.00 Å are shown.)

I^- No.	Occupancy	B_{eq} (Å^2)	Trp	I···N (Å)	I···H (Å)	I···H—N (°)	Water No.	I···H_2O (Å)	I	I···I (Å)
21	0.27	21.44	311	3.56	2.74	159.6	81	1.55		
22	0.42	13.62	115	3.43	2.69	145.6	82	0.24	26	2.10
			209	3.70	2.94	147.8				
			313	3.89	3.24	134.0	86	2.59		
			113	3.77	3.24	122.3				
23	0.08	12.59	413	3.31	2.58	144.3	83	0.54	24	0.95
			415	3.66	2.88	151.7	84	0.60		
24	0.10	15.12	415	3.93	3.13	156.4	83	1.04		
			413	3.90	3.08	159.8	23	0.95		
25	0.12	23.66	Ala405	3.71	2.89	160.6	85	0.83		
							92	3.45		
26	0.09	23.91	115	3.29	2.74	122.8	86	0.81		
			315	3.53	2.89	132.8				
			113	3.61	2.87	146.1	82	2.28	22	2.10
27	0.13	26.55	213a	3.41	2.65	148.4	88	2.84		
			215b	3.64	2.82	160.6				

Table 7
Orientations of side chains in crystal structures of the gD–NaI complex.

In the case of two positions being occupied by a side chain, the conformation with lower occupancy is shown in parentheses. Cases of similar torsion angles defining the conformations are marked with asterisks. The order of strands has been changed to highlight similarities and differences between them. To make the analysis clearer, we have used the older *gauche–trans* notation and to avoid ambiguity in the χ_1 torsion angle used for the $N-C^{\alpha}-C^{\beta}-CH_3$ angle (IUPAC–IUB Commission on Biochemical Nomenclature, 1970), in the case of Val having two undistinguished methyl groups the irregular torsion angle $N-C^{\alpha}-C^{\beta}-H$ is shown instead.

Residue	Strand 100	Strand 300	Strand 200	Strand 400
Val1	g^-	g^-	g^+	g^+
D-Leu4	g^+	g^+* (41%)	g^+	g^+
D-Val6	g^- (g^+ 27%)	g^- (t 34%)	t (g 49%)	g^+ (t 32%)
Val7	t	t	g^- (t 40%)	t (g^+ 36%)
D-Val8	g^+ (g^- 36%)	g^+ (t 46%)	g^+	g^+* (26%)
Trp9	g^-* (41%)	g^-	g^-	g^-* (41%)
D-Leu10	g^+ (g^- 48%)	g^+	g^-	g^-* (46%)
Trp11/Phe	g^-	g^-	g^-* (39%)	g^-* (38%)
D-Leu12	t	t	g^+ (g^- 40%)	g^-
Trp13	t	t	g^-* (34%)	g^-
D-Leu14	t	t	g^- (g^+ 41%)	g^-
Trp15	t	t	g^-* (15%)	g^-

The relatively small Na^+ ions in the current antiparallel double-stranded gramicidin dimer structure make fewer contacts with carbonyl groups in the channel wall (Table 4 and Fig. 4) compared with the previously bound alkali-metal ions. The smaller size of sodium allows only three $Na^+\cdots$ carbonyl contacts (two of which are $Na^+\cdots O$ and one is $Na^+\cdots\pi$ type) owing to the closer proximity of the ion to the channel wall (Fig. 5).

3.4. Interchannel space

The total iodine occupancy in the asymmetric unit is 1.21 (Table 5), which is very close to the sum of occupancies of 1.26 observed for sodium (Table 3). In addition to the seven anionic sites grouped into four distinct positions and identified with high certainty owing to the large anomalous signal of the iodine ($f''_{0.918}$ = 2.88 e), there are at least 14 water sites occupied by a total of 7.88 molecules and three methanol sites in the inter-channel space (Table 5). All iodides form hydrogen bonds to Trp side chains (and possibly with water), except for I25, which is hydrogen bonded to the main-chain NH group of Ala405, a phenomenon that was not observed in other iodide complexes of gramicidin structures (Table 6). Some waters are very close to the iodides, excluding their simultaneous presence. This observation was taken into account in the refinement process of the respective occupancy factors.

3.5. Conformations of side chains

The orientations of Val, Leu and Trp side chains follow a striking regularity in this heterogenic gramicidin complex crystal (Table 7). The relative interaction between these side chains determines their spatial arrangement, which is especially apparent in the sequence 9–15, where large but flat Trp and bulky Leu residues are grouped alternately. The other end of the gramicidin chain is mostly occupied by residues with smaller side chains, with the largest being a stretch of four Val side chains in a row. The alternate arrangement of L- and D-amino acids secures the helical conformation of the two peptide chains intertwined in dimers owing to the presence of all of the side chains on the same side, while smaller side chains in one half of the molecule ease possible repulsions in the helical dimers being formed owing to a regular pattern of possible intermolecular hydrogen bonds.

Two distinct patterns of side-chain orientations are readily apparent in Table 7, which presumably results from the relative dimer and strand compositions (§3.1). Similar side-chain conformations are found in strands 100 and 300 as well as in strands 200 and 400. Conversely, very different side-chain conformations are found when comparing strands belonging to the same dimer.

3.6. Iodide occupancy factors based on anomalous scattering

As in our previous study on complexed gramicidin structures (Olczak *et al.*, 2007), one of our aims was the precise determination of ion occupancies. Refinement of these parameters can be ambiguous in cases in which the same sites are shared by other moieties such as water (this also applies to iodide anions and sodium cations). Unfortunately, analysis is limited by the fact that only iodide anions are visible in the anomalous difference maps.

To cross-check that the occupancy parameters of anomalous scatterers were correctly determined, we analyzed various characteristics based on resonant scattering, including the anomalous signal ($\Delta_{anom} = \langle|\Delta F|\rangle/\langle F\rangle$), the correlation between the refined occupancies of anomalous scatterers and

the maxima on anomalous difference maps (Fig. 6) and the Flack parameter (Flack, 1983).

The value of $\Delta_{\rm anom,observed}$ for the studied structure obtained on the basis of observed structure factors is equal to 3.3%. The value $\Delta_{\rm anom,observed}$ is often treated as an actual anomalous signal $\Delta_{\rm anom}$, but the experimental differences ΔF, in addition to the anomalous differences $\Delta F_{\rm anom}$, also contain measurement uncertainties $\Delta F_{\rm err}$: $\Delta F = \Delta F_{\rm anom} + \Delta F_{\rm err}$. The experimental error contribution to $\Delta_{\rm anom,observed}$ (estimated from the reflection uncertainty σ) equals 2.7%. Consequently, the actual anomalous signal $\Delta_{\rm anom}$ can be estimated to be about 1.9% $\{\Delta_{\rm anom} = [(\Delta_{\rm anom,observed})^2 - (\Delta_{\rm error})^2]^{1/2}\}$.

If our model is correct, this experimentally obtained result should be consistent with predictions based on that model. In the case of the gD–NaI complex studied here $\Delta_{\rm anom}$ (obtained from the calculated structure factors $F_{\rm c}$) equals 1.8%, which is in very good agreement with the experimental value of 1.9%.

Even if a three-dimensional model of a given structure is not known, $\Delta_{\rm anom}$ can be estimated on the basis of the composition of that structure. This can be performed with the help of the following formula [which is an obvious generalization of the formulae presented in Olczak *et al.* (2003, 2007) and Olczak (2004), with a correction for centrosymmetric substructure introduced by Flack & Shmueli (2007)],

$$\Delta_{\rm anom} = \left[\sum_{A>B}^{Q} (\Delta_{\rm anom}^{AB})^2 - \sum_{A'>B'}^{Q'} (\Delta_{\rm anom}^{A'B'})^2 \right]^{1/2}, \qquad (1)$$

where

$$\Delta_{\rm anom}^{AB} = \frac{8}{\pi^{3/2}} \frac{|f_B''(f_A + f_A') - f_A''(f_B + f_B')|}{\langle |F| \rangle^2} \left(\sum_{j=1}^{N_A} \sum_{i=1}^{N_B} c_{A_j}^2 c_{B_i}^2 \right)^{1/2},$$

A and B denote atom types, A' and B' denote atom types arranged in centrosymmetric substructure, N_A and N_B are the number of atoms of types A and B, respectively, and the c values are occupancy factors. ($\Delta_{\rm anom}$ can be calculated using this formula on the webpage http://assc.p.lodz.pl.)

The value obtained from this formula for the gD–NaI complex is 1.43%, which is a significant variation from the experimental value of 1.9%. This discrepancy most probably arises from the assumption made in the derivation of (1), namely that atoms are evenly distributed in the unit cell. This is not strictly fulfilled in this particular case [a channel-like structure with no uniform distribution of electron density along the channel axis and anomalous scatterers (iodides) placed outside the channel].

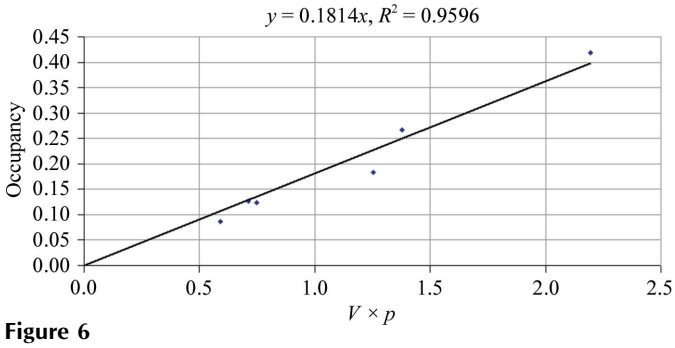

Figure 6
Correlation between $V \times p$ and occupancy factors of anomalously scattering iodine ions. V is the volume, calculated as $(4/3)\pi(U_{11}U_{22}U_{33})^{1/2}$, where U_{11}, U_{22} and U_{33} are components of the diagonalized displacement tensor and p is a maximum on the anomalous difference density map.

The analysis of the anomalous signal helps to bolster any conclusions drawn from the refined occupancy factors of anomalous scatterers. This refinement is potentially error-prone and can lead to erroneous conclusions, as was the case with the gA–CsCl structure (Wallace *et al.*, 1990). The authors reported that the experimental anomalous signal $\Delta_{\rm anom,observed}$ was 5.6% (in fact, the authors reported $\langle|\Delta F^2|\rangle/\langle F^2\rangle$ and we recalculated this value to obtain $\Delta_{\rm anom,observed}$). As mentioned above, the actual anomalous signal $\Delta_{\rm anom}$ should be lower (usually quite significantly) because of experimental uncertainty. Surprisingly, the expected anomalous signal, $\Delta_{\rm anom}$, calculated using (1) on the basis of the reported occupancies of Cs^+ and Cl^- ions was 9.8% and the anomalous signal determined directly from calculated structure factors ($F_{\rm c}$) for the refined model was 9%. The last two values are in a good agreement with each other, which confirms the usefulness of (1) for estimating the actual anomalous signal. However, they are significantly greater than the experimental value (5.6%), leading to a considerable overestimation of ion occupancies in the gA–CsCl complex.

Another test that we used to confirm the correctness of the anomalous substructure in the gD–NaI complex was the correlation between the freely refined occupancies of iodide anions (shared with water molecules) with the product of the 'volume' and the height of the respective peaks in the anomalous difference maps (Fig. 6). The anomalous difference maps (ΔF, $\varphi_{\rm calc} - 90^\circ$) were prepared with phases $\varphi_{\rm calc}$ calculated for the gramicidin structure alone (no waters or any other molecules) and revealed all seven iodide sites. The high correlation factor of $R^2 = 0.96$ (Fig. 6) indicated that relative occupancies are correctly assigned to iodide ions.

As explained in Olczak *et al.* (2007), having established the relative occupancies of anomalous scatterers, the Flack parameter can be used as an indicator of the correctness of the global occupancy of the anomalous substructure. For the structure of gD–NaI it is equal to 0.06 (3), which is close enough to zero to confirm the correctness of the anomalous substructure.

Partial financial support from the Polish Committee for Scientific Research under project 3 T09A 047 26 (2004–2006) is gratefully acknowledged (MLG and MS). Portions of this work were performed at DND-CAT located at Sector 5 and at LS-CAT located at Sector 21 of the Advanced Photon Source (APS). DND-CAT is supported by E. I. DuPont de Nemours & Co., The Dow Chemical Company and the State of Illinois. LS-CAT was supported by the Michigan Economic Development Corporation and the Michigan Technology Tri-Corridor for the support of this research program (Grant 085P1000817). Use of the APS was supported by the US Department of

Energy, Office of Science, Office of Basic Energy Sciences under Contract No. DE-AC02-06CH11357.

References

Allen, F. H. (2002). *Acta Cryst.* B**58**, 380–388.
Burkhart, B. M., Gassman, R. M., Langs, D. A., Pangborn, W. A. & Duax, W. L. (1998). *Biophys. J.* **75**, 2135–2146.
Burkhart, B. M., Li, N., Langs, D. A., Pangborn, W. A. & Duax, W. L. (1998). *Proc. Natl Acad. Sci. USA*, **95**, 12950–12955.
Chen, Y., Tucker, A. & Wallace, B. A. (1996). *J. Mol Biol.* **264**, 757–769.
Doyle, D. A. & Wallace, B. A. (1997). *J. Mol. Biol.* **266**, 963–977.
Duax, W. L., Pletnev, V. & Burkhart, B. M. (2003). *J. Mol. Struct.* **647**, 97–111.
Dubos, R. J. (1939). *J. Exp. Med.* **70**, 1–10.
Engh, R. A. & Huber, R. (1991). *Acta Cryst.* A**47**, 392–400.
Flack, H. D. (1983). *Acta Cryst.* A**39**, 876–881.
Flack, H. D. & Shmueli, U. (2007). *Acta Cryst.* A**63**, 257–265.
Główka, M. L., Olczak, A., Bojarska, J., Szczesio, M., Duax, W. L., Burkhart, B. M., Pangborn, W. A., Langs, D. A. & Wawrzak, Z. (2005). *Acta Cryst.* D**61**, 433–441.
Gross, E. & Witkop, B. (1965). *Biochemistry*, **4**, 2495–2501.
Hotchkiss, R. D. (1944). *Adv. Enzymol.* **4**, 153–199.
Hotchkiss, R. D. & Dubos, R. J. (1940). *J. Biol. Chem.* **132**, 791–792.
Hotchkiss, R. D. & Dubos, R. J. (1941). *J. Biol. Chem.* **141**, 155–162.
Ishii, S. & Witkop, B. (1963). *J. Am. Chem. Soc.* **85**, 1832–1834.
IUPAC–IUB Commission on Biochemical Nomenclature (1970). *Biochemistry*, **9**, 3471–3479.
Langs, D. A. (1988). *Science*, **241**, 188–191.
Langs, D. A., Smith, G. D., Courseille, C., Précigoux, G. & Hospital, M. (1991). *Proc. Natl Acad. Sci. USA*, **88**, 5345–5349.
Olczak, A. (2004). *46th Polish Crystallographic Meeting*, p. 16.
Olczak, A., Cianci, M., Hao, Q., Rizkallah, P. J., Raftery, J. & Helliwell, J. R. (2003). *Acta Cryst.* A**59**, 327–334.
Olczak, A., Główka, M. L., Szczesio, M., Bojarska, J., Duax, W. L., Burkhart, B. M. & Wawrzak, Z. (2007). *Acta Cryst.* D**63**, 319–327.
Otwinowski, Z. & Minor, W. (1997). *Methods Enzymol.* **276**, 307–326.
Pressman, B. C. (1965). *Proc. Natl Acad. Sci. USA*, **53**, 1076–1083.
Ramachandran, L. K. (1963). *Biochemistry*, **2**, 1138–1142.
Sarges, R. & Witkop, B. (1964). *J. Am. Chem. Soc.* **86**, 1862–1863.
Sarges, R. & Witkop, B. (1965). *J. Am. Chem. Soc.* **87**, 2011–2020.
Sheldrick, G. M. (2008). *Acta Cryst.* A**64**, 112–122.
Urry, D. W. (1971). *Proc. Natl Acad. Sci. USA*, **68**, 672–678.
Urry, D. W., Goodall, M. C., Glickson, J. D. & Mayers, D. F. (1971). *Proc. Natl Acad. Sci. USA*, **68**, 1907–1911.
Veatch, W. R. & Blout, E. R. (1974). *Biochemistry*, **13**, 5257–5264.
Veatch, W. R., Fossel, E. T. & Blout, E. R. (1974). *Biochemistry*, **13**, 5249–5256.
Wallace, B. A., Hendrickson, W. A. & Ravikumar, K. (1990). *Acta Cryst.* B**46**, 440–446.
Wallace, B. A. & Ravikumar, K. (1988). *Science*, **241**, 182–187.